

Activation of Group I and Group II Metabotropic Glutamate Receptors Causes LTD and LTP of Electrical Synapses in the Rat Thalamic Reticular Nucleus

Zemin Wang,^{1,2} Ryan Neely,² and Carole E. Landisman^{1,2}

¹Department of Neurology, Boston Children's Hospital, Boston, Massachusetts 02115, and ²Center for Brain Science, Harvard University, Cambridge, Massachusetts 02138

Compared with the extensive characterization of chemical synaptic plasticity, electrical synaptic plasticity remains poorly understood. Electrical synapses are strong and prevalent among the GABAergic neurons of the rodent thalamic reticular nucleus. Using paired whole-cell recordings, we show that activation of Group I metabotropic glutamate receptors (mGluRs) induces long-term depression of electrical synapses. Conversely, activation of the Group II mGluR, mGluR3, induces long-term potentiation of electrical synapses. By testing downstream targets, we show that modifications induced by both mGluR groups converge on the same signaling cascade—adenylyl cyclase to cAMP to protein kinase A—but with opposing effects. Furthermore, the magnitude of modification is inversely correlated to baseline coupling strength. Thus, electrical synapses, like their chemical counterparts, undergo both strengthening and weakening forms of plasticity, which should play a significant role in thalamocortical function.

Key words: electrical synapses; gap junctions; mGluRs; synaptic plasticity

Introduction

Electrical synapses (gap junctions) are widespread throughout the mammalian brain (Bennett and Zukin, 2004; Connors and Long, 2004; Söhl et al., 2005). The thalamic reticular nucleus (TRN) is composed of GABAergic inhibitory neurons that communicate among each other primarily via gap junctional synapses (Landisman et al., 2002). More than 50% of closely apposed TRN neurons interact via electrical synapses (Landisman et al., 2002; Long et al., 2004) and <1% of these coupled neuronal pairs use GABAergic inhibitory chemical communication (Landisman et al., 2002). The TRN receives excitatory glutamatergic input from corticothalamic (CT) and thalamocortical (TC) axons and projects all of its inhibitory efferent fibers to the thalamic relay nuclei (Scheibel and Scheibel, 1966; Steriade et al., 1997; Crabtree, 1999; Deleuze and Huguenard, 2006). Within the TRN, activation of metabotropic glutamate receptors (mGluRs), either by briefly tetanizing CT feedback fibers or by applying the nonspecific mGluR agonist 1-aminocyclopentane-1,3-dicarboxylic acid (ACPD), causes long-term depression of electrical synapses (eLTD; Landisman and Connors, 2005). However, the underlying mechanisms of this plasticity are still unknown.

mGluRs are G-protein-coupled receptors, and the TRN has significant expression of group I and group II proteins (Loureño

Neto et al., 2000). Generally, group II mGluRs (mGluR2 and mGluR3) couple to Gi/o protein, which decreases cAMP accumulation by inhibition of adenylyl cyclase (AC; Coutinho and Knöpfel, 2002). Group I mGluRs (mGluR1 and mGluR5), meanwhile, couple to either Gq protein, which activates protein kinase C (PKC) by phospholipase C (PLC), or they couple to Gs, which activates protein kinase A (PKA) by increasing cAMP production (Coutinho and Knöpfel, 2002; Kim et al., 2008). Activation of group I mGluRs leads to an increase in membrane input resistance (R_{in}) and depolarization of TRN neurons, whereas activation of group II (mGluR3) causes a decrease in R_{in} and hyperpolarization (Cox and Sherman, 1999; Alexander and Godwin, 2006). Both studies demonstrate that these changes to R_{in} and membrane voltage (V_m) are due to changes in potassium conductances.

The nonspecific mGluR agonist ACPD causes eLTD in the TRN (Landisman and Connors, 2005). Hughes and Crunelli (2006) suggested that group I and group II mGluRs could induce electrical synaptic plasticity in the TRN by phosphorylating and dephosphorylating gap junction proteins, respectively. This would be achieved by activation of groups I and II converging on the same intracellular signaling pathway (AC–cAMP–PKA), but with opposing modulatory effects (Fig. 1). However, the specific mGluRs involved in gap junctional long-term plasticity have not been demonstrated.

To study the potential signaling cascades underlying the long-term modification of electrical synapses in TRN neurons, we used dual whole-cell recordings in rat TC slices (Fig. 1A,B) combined with pharmacology. Our results indicate that activation of group I mGluRs causes eLTD. Conversely, activation of mGluR3 (group II) induces long-term potentiation of electrical synapses (eLTP).

Received Sept. 3, 2014; revised March 19, 2015; accepted March 20, 2015.

Author contributions: Z.W. and C.E.L. designed research; Z.W. and R.N. performed research; Z.W. analyzed data; Z.W. and C.E.L. wrote the paper.

This work was supported by the Milton Fund, Harvard University.

The authors declare no competing financial interests.

Correspondence should be addressed to Carole E. Landisman at the address. E-mail: carole.landisman@gmail.com.

DOI:10.1523/JNEUROSCI.3688-14.2015

Copyright © 2015 the authors 0270-6474/15/357616-10\$15.00/0

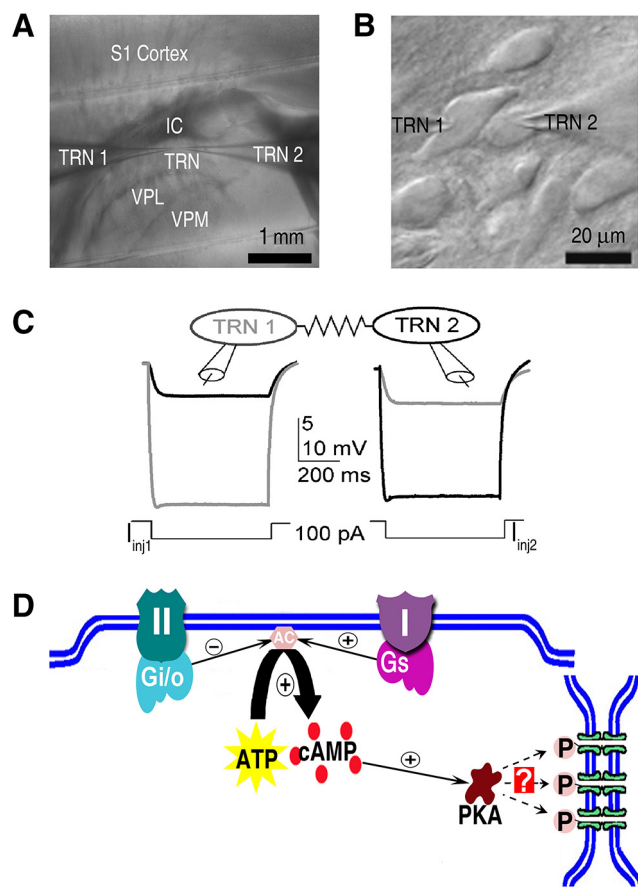


Figure 1. Experimental methods and design. **A**, Low-magnification infrared differential interference contrast image of TC slice preparation with two recording electrodes in the TRN and their respective recorded somata, labeled TRN 1 and TRN 2. IC, Internal capsule; VPL, ventral posterolateral nucleus; VPM, ventral posteromedial nucleus; S1 cortex, primary somatosensory cortex. **B**, High-magnification image showing an electrically coupled pair of neurons in the TRN with their whole-cell recording electrodes. **C**, Schematic of an electrically coupled pair of TRN neurons with their recording electrodes and their voltage responses to alternating hyperpolarizing current (I_{inj}) injected to each cell. The passive resistor is used as a symbol for the gap junctional (electrical) synapse. During I_{inj1} , TRN 1 responded with a direct voltage deflection (left gray trace), and TRN 2 responded passively through the gap junctional synapse (left black trace). On the right is the reverse: TRN 2 received direct stimulation (black trace), and TRN 1 responded via the gap junctional synapse. Voltage traces from an actual recorded pair. **D**, Schematic diagram showing metabotropic glutamatergic (mGluR) G-protein-coupled signal cascades involved in the modulation of gap junctional synapses. Activation of group I (plum) and group II (teal) mGluRs, via Gs (purple), or Gi/o (aqua) proteins respectively converge on the same intracellular signaling pathway. ATP, Adenosine triphosphate. The question mark indicates the unknown effect on gap junctional strength of PKA phosphorylation.

To our knowledge, this is the first electrophysiological evidence of mGluR activation inducing eLTP. Both mGluR-dependent eLTD and eLTP involve the same signaling cascade, AC–cAMP–PKA, but with opposing actions. Finally, the magnitude of the induced modification of electrical synapses was found to be inversely related to baseline coupling strength.

Materials and Methods

Slice preparation. TC slices were taken from Sprague Dawley rats of either sex, as described previously (Agmon and Connors, 1991). All experimental procedures were approved by Harvard University and were performed in accordance with guidelines of the National Institutes of Health. Briefly, rats, age 11–14 postnatal days, were killed with isoflurane and quickly decapitated. The brains were then extracted and submerged in 305 mOsm, 0–4°C slicing solution (in mM: 72 sucrose, 83 NaCl, 2.5

KCl, 1 NaH_2PO_4 , 3.3 $\text{MgSO}_4 \cdot 7\text{H}_2\text{O}$, 26.2 NaHCO_3 , 22 dextrose, and 0.5 CaCl_2) saturated with 95% O_2 and 5% CO_2 . TC slices 400 μm thick were cut using a Vibroslice (World Precision Instruments). The slices were incubated in the same oxygenated slicing solution for 20 min, and then held at room temperature for another 30 min before recording. Slices remained viable for recording for 4–6 h.

Dual whole-cell recording. Prepared TC slices were transferred to a recording chamber superfused with artificial CSF (ACSF), containing the following (in mM): 126 NaCl, 3 KCl, 1.25 NaH_2PO_4 , 2 $\text{MgSO}_4 \cdot 7\text{H}_2\text{O}$, 26 NaHCO_3 , 10 dextrose, and 2 CaCl_2 . The ACSF was adjusted to ~ 305 mOsm and pH ~ 7.2 at $34 \pm 0.5^\circ\text{C}$, saturated with oxygen and was bubbled with 95% oxygen/5% CO_2 . The chamber was superfused at a rate of 2 ml/min. Slices were visualized using an Olympus Optical BX50WI microscope with a QImaging CCD camera, using infrared differential interference contrast while in the submerged recording chamber.

Whole-cell recording pipettes were pulled from borosilicate glass on a P-97 micropipette puller (Sutter Instruments) and had resistances of 5–7 $\text{M}\Omega$. mGluRs are known to modulate potassium channels, which in turn can change R_{in} and V_m (Golshani et al., 1998; Cox and Sherman, 1999; Alexander and Godwin, 2005). To prevent these changes, we used cesium-based internal solution in the recording electrodes for experiments involving mGluRs and their coupled G-proteins. The internal solution contained the following (in mM): 120 CsOH, 120 gluconic acid, 10 HEPES, 0.2 EGTA, 2 MgCl_2 , 0.1 CaCl_2 , 4 NaCl, 4 ATP-Mg, 0.3 GTP-Tris, 10 phosphocreatine-Tris, and 5 QX-314. pH was adjusted to 7.25 with CsOH, and osmolality was 290 mOsm. Thus, the CsOH and QX-314 effectively blocked potassium and sodium channels so that R_{in} and V_m remained constant before and after drug washes. In addition, we used holding current to ensure that V_m was stable throughout all recordings. For the remaining experiments, recording electrodes were filled with potassium gluconate internal solution, which contained the following (in mM): 135 K-gluconate, 2 KCl, 4 NaCl, 2 MgCl_2 , 0.1 CaCl_2 , 10 HEPES, 0.2 EGTA, 4 ATP-Mg, 0.3 GTP-Tris, and 10 phosphocreatine-Tris. Osmolality was adjusted to ~ 290 mOsm, and pH was adjusted to 7.25 using 1 M CsOH.

Isolating the activity of electrical synapses. To isolate the activity of electrical synapses from those of chemical synapses, the antagonists DNQX (20 μM) and APV (50 μM) were used to silence glutamatergic AMPA and NMDA transmission, respectively. Additionally, V_m was held constant at -70 mV with current injection for the duration of each experiment to avoid changes in R_{in} due to the activation or inactivation of voltage-dependent ion channels.

We did not observe GABAergic transmission between electrically coupled TRN cells, presumably because these synapses are extremely rare for closely apposed TRN cells (Landisman et al., 2002; Long et al., 2004; but see Deleuze and Huguenard, 2006), so we did not use specific GABA blockers. In addition to blocking K^+ channels, cesium and QX-314 also block potassium channels and GABA $_B$ receptors (McLean et al., 1996). Thus with chemical transmission removed, and sodium and potassium channels blocked, we were able to determine that any changes we measured after introducing the various pharmacological agents were due exclusively to changes in electrical coupling strength.

Isolating the effects of specific mGluRs. Since NAAG is an endogenous peptide expressed in TRN neurons (Henderson and Salt, 1988; Moffett and Namboodiri, 2006) and can be hydrolyzed into glutamate and N-acetylaspartate by the enzyme N-acetyl-alpha-linked-acidic-dipeptidase (NAALADase; Fuhrman et al., 1994), we added mGluR antagonists to the bath solution to block non-group II mGluRs: the mGluR1 antagonist 7-(hydroxyimino)cyclopropa[b] chroma-1a-carboxylate ethyl ester (CPCOEt; 50 μM), the mGluR5 antagonist MPEP (20 μM), and the group III mGluR antagonist MAP4 (200 μM).

Data acquisition and analysis. The two recording electrodes were controlled by Patchstar micromanipulators (Scientifica). After whole-cell patching, electrophysiological signals were recorded in current clamp using Axoprobe-1A amplifiers (Molecular Devices). Axoprobe data were digitized with a Digidata 1322A analog to digital converter (Molecular Devices). Data were acquired and stored using Clampex 9.0 software (Molecular Devices).

The reported coupling coefficient (cc) and average baseline coupling strength [coupling conductance (G_C); explained below] are the average values obtained from voltage responses to 5–10 sets of alternating hyperpolarizing current stimuli. Each group of the 5–10 sets of stimulus–response data was collected every 2 min. The pooled data are expressed as means \pm SE. Statistical analyses included two-tailed paired t tests and one-tailed unpaired t tests. More specifically, each set of time-course data from a single pair of neurons was analyzed using one-tailed unpaired t tests to determine whether responses following the offset of drug washes showed significant changes in gap junctional conductance compared with the baseline G_C : [data binned for time points during 10 min before drug wash] versus [data binned for time points 20–30 min after the start of the drug wash]. Then, a single value for each neuronal pair was calculated as a percentage change in baseline conductance.

For population analyses, data from each neuronal pair were collapsed into two values: (1) the average baseline coupling strength (G_C) for the 10 min before drug wash and (2) the average G_C for 20–30 min after drug wash. Each group of paired datasets for a specific drug wash was then tested using a two-tailed paired t test to determine whether each drug caused significant changes in coupling strength over a population of recorded pairs.

Coupling strength collection and measurement. To measure electrical synaptic strength, alternating hyperpolarizing current steps (100 pA, 600 ms, 1 s interstimulus intervals) were injected into each cell 5–10 times every 2 min before, during, and after drug application (Fig. 1C).

Voltage responses of both cells were collected and stored before, during, and after drug application. Stored data were analyzed using Matlab to measure gap junctional coupling strength and R_{in} .

R_{in} was measured as $R_{in} = \Delta V / I_{inj}$, where ΔV is the average voltage response of a neuron to injected current, I_{inj} . R_{in} was monitored during the entire experimental period. Data were discarded if access resistance change was $\geq 15\%$ during recording. It should be noted that no consistent changes in R_{in} were observed following drug washes. The average R_{in} over the population recorded with the cesium-based internal solution was 342 M Ω pretest ($n = 82$). The average R_{in} of neurons recorded with K-gluconate internal solution was 162 M Ω pretest ($n = 64$).

The cc is a ratio of the postsynaptic (passive) voltage change (ΔV_2) divided by presynaptic voltage response (ΔV_1) due to current injection, under steady-state conditions. Thus the equation for cc is as follows: $cc_{12} = \Delta V_2 / \Delta V_1$.

Because electrical synapses are bidirectional, and current steps were alternately delivered to each cell of a pair, the reported cc is the mean value of cc calculated for each direction as follows: $cc_{ave} = (cc_{12} + cc_{21}) / 2 = [(\Delta V_2 / \Delta V_1) + (\Delta V_1 / \Delta V_2)] / 2$.

Although cc measures the fraction of the signal conveyed through electrical synapses, it is subject to the influence of the R_{in} of the two coupled cells, and is thus not an accurate measure of the strength of the gap junctional synapse. The electrical G_C , however, gives an accurate measure of the strength of the isolated gap junction (Bennett, 1966). The calculation of the G_C is based on a circuit model of two isopotential neurons connected by a single electrical junction (Bennett, 1966). G_C is estimated for each direction of current flow in a cell pair as follows:

The transfer resistance (R_{12}) is a measure of the passive voltage response in one cell resulting from current injected into the other cell: $R_{12} = R_{21} = \Delta V_2 / I_{inj1} = \Delta V_1 / I_{inj2}$.

$G_C = 1/R_C$ where $R_C = (R_1 R_2 - R_{12}^2) / R_{12}$, where R_1 is the R_{in} of cell 1, and R_2 is the R_{in} of cell 2. Thus, $G_C = 1/R_C$.

Results

Activation of mGluR3 (group II) induces eLTP in TRN cells

To explore mGluR receptor specificity responsible for plasticity, we targeted specific receptors with the highest expression patterns in the TRN, starting with mGluR3, a subtype of group II mGluRs (Ohishi et al., 1993; Lourenço Neto et al., 2000; Tamaru et al., 2001). Since it has been previously demonstrated that activation of groups I and II mGluRs change potassium conductances, causing changes in V_m and R_{in} , we blocked K-channels by using cesium and QX-314 in our recording electrodes.

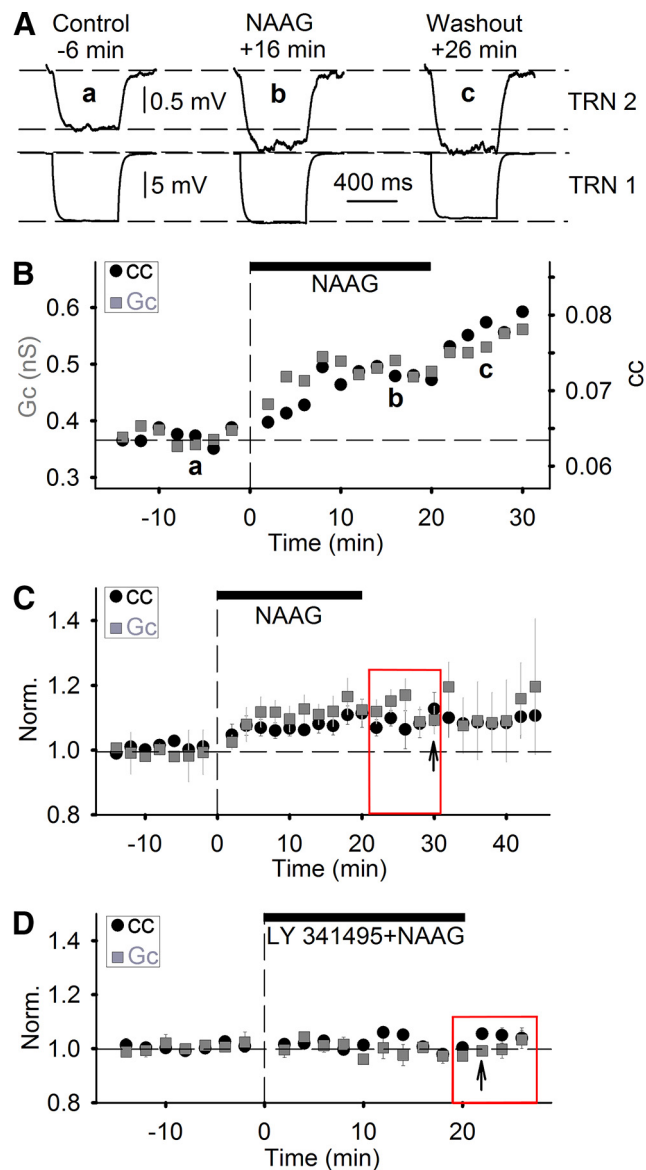


Figure 2. mGluR3 agonist NAAG induces eLTP of electrical synapses in the TRN. **A**, Example single traces from a pair of coupled TRN neurons before (*a*), during (*b*), and after (*c*) NAAG application (400 μ M, 20 min). TRN 1 (bottom traces) received a hyperpolarizing current injection (−100 pA, 600 ms), which induced a gap junctional response in TRN 2 (top traces). **B**, Time course measurements of cc (black solid circles) and G_C (gray squares) for the pair shown in **A** (*a–c* mark the time points that correspond to the traces in **A**). **C**, Population time course for cc and G_C (mean \pm SE; $n = 11$ pairs; cc $p = 0.04$, G_C $p = 0.004$) before, during, and after NAAG application. Y values are normalized to the average value of all baseline time points. X values are binned every 2 min, and each time-point value is based on an average of 5–10 trials. 0 min = start of drug wash. Black bars indicate duration of drug application. Arrow denotes $n = 3$ pairs for ≥ 30 min (30–44 min). **D**, Normalized population time course for cc and G_C ($n = 9$ pairs) before, during, and after the group II mGluR antagonist LY 341495 (1 μ M, 20 min) with NAAG application. Arrow indicates $n = 2$ pairs for last three time points (22–26 min). Red boxes in **C** and **D** indicate the data points used to calculate the change in strength compared with the pre-drug baselines.

We bath-applied the selective mGluR3 agonist NAAG (Fig. 2A). In 11 electrically coupled pairs, baseline coupling strength was stable (Fig. 2B,C). Though the voltage response of the current-injected cell did not change significantly following NAAG application (Fig. 2A, TRN 1), the electrical synaptic voltage responses in the coupled cell increased significantly (Fig. 2A, TRN 2, B,C). Coupling strength potentiation reached steady-

state values ~ 10 min after drug application (Fig. 2C). Because NAAG washes out extremely quickly—on the order of seconds (Westbrook et al., 1986; Kolodziejczyk et al., 2009)—these effects are consistent with long-term plasticity. Over the entire population, G_C increased $14 \pm 4\%$ (mean \pm SE; $n = 11$ pairs, $p = 0.004$, two-tailed paired t test). Of the 11 pairs tested, seven showed significant potentiation (one-tailed unpaired t tests). Thus, activation of mGluR3 causes eLTP in the TRN.

To further confirm that the eLTP effects of NAAG were caused by mGluR3 receptor activation, the experiments were repeated in the presence of the group II mGluR antagonist LY 341495. Of the nine coupled pairs tested, none showed significant changes in coupling strength: $\Delta G_C = 0.7 \pm 4.4\%$ ($p = 0.88$; Fig. 2D).

Activation of group I mGluRs causes eLTD

Groups I and II mGluRs have been shown to have opposite effects on TRN neuronal excitability and R_{in} (Cox and Sherman, 1999). Also, group I mGluRs converge on the same signaling cascade as the group II receptors (Fig. 1D). Combining these results, we hypothesized that group I receptors might also be involved in gap junctional plasticity.

We applied the group I mGluR agonist (*RS*)-3,5-dihydroxyphenylglycine (DHPG) to test its effect on electrical coupling strength. Note that R_{in} remained stable before versus after DHPG application (Fig. 3A, TRN 1). The passive voltage responses of the electrically coupled neighbor, however, decreased significantly 2–5 min following drug application and remained depressed for the remainder of the recording period (Fig. 3A, TRN 2, B). For the population of pairs tested with DHPG, coupling strength depressed significantly: $\Delta G_C = -23 \pm 6\%$ ($n = 11$ pairs; $p = 0.004$, two-tailed paired t test; Fig. 3C). Of the 11 pairs tested, eight showed significant depression (one-tailed unpaired t tests). These results suggest that activation of group I mGluRs causes significant eLTD between electrically coupled TRN neurons.

Gi/o protein plays an important role in eLTP

Because group II mGluRs are primarily linked to Gi/o protein (Pin and Acher, 2002), we reasoned that increasing Gi/o protein activity could mediate the long-term modification induced by group II mGluR activation. We selected mastoparan, a peptide activator of Gi/o (Shpakov and Pertseva, 2006), to test whether it could mimic the effect of NAAG on electrical synaptic strength. After mastoparan application, electrical coupling strength potentiated significantly (Fig. 4A–C): $\Delta G_C = 18 \pm 6\%$ ($n = 10$ pairs, $p = 0.03$, two-tailed paired t test); and of the 10 pairs tested, eight showed significant eLTP (one-tailed unpaired t tests). This effect continued throughout the entire recording period, long after washout. These results strongly suggest that the induction of eLTP in the TRN via activation of mGluR3 is mediated by Gi/o protein.

Activation of AC induces eLTD

Although group I mGluRs are dominantly linked to Gq protein, which activates PLC and generates PKC (Conn and Pin, 1997; Coutinho and Knöpfel, 2002; Kim et al., 2008), in some cases, group I mGluRs also couple to Gs (Hermans and Challiss, 2001; Tateyama and Kubo, 2007), which increases PKA activity (Bandrowski et al., 2001; Fig. 1D). Thus, group I and group II mGluRs can converge on the AC–cAMP–PKA signaling pathway (Hughes and Crunelli, 2006). However, due to the lack of a rapid and effective agonist for Gs, we were unable to test its role in the

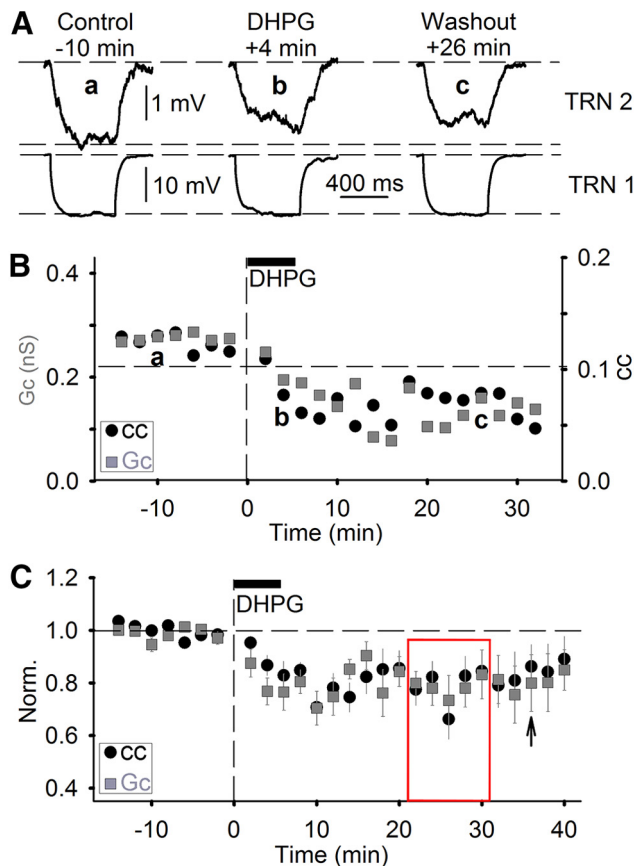


Figure 3. Group I mGluR agonist DHPG induces eLTD of electrical synaptic coupling strength. **A**, Example single traces of a coupled pair before (*a*), during (*b*), and after (*c*) DHPG application (50 μ M, 5 min); same layout as in Figure 2A. **B**, Time course measurements of cc (black solid circles) and G_C (gray squares) for the pair shown in **A** (*a–c* mark the time points that correspond to the traces in **A**). **C**, Normalized population time course for cc and G_C before, during, and after DHPG application (mean \pm SE; $n = 11$ pairs; cc $p = 0.004$, G_C $p = 0.004$). Arrow indicates $n = 4$ pairs for last three time points (36–40 min). Red box indicates regions of analysis following drug washout.

induction of eLTD directly. Instead we examined the role of AC, the downstream substrate of Gs (and Gi/o).

It has been reported that activation of AC intracellularly has varying effects on gap junctional coupling and conductance. In rabbit retinal amacrine cells and rat prefrontal cortex, incubation in the cell-permeable AC activator forskolin decreases dye coupling (Hampson et al., 1992; Rörig et al., 1995). Similarly, in rat hippocampus, forskolin, while in the bath, decreases electrical coupling between interneurons (Zsiris and Maccaferri, 2008). Conversely, in hippocampal CA3 pyramidal cells, forskolin increases electrical coupling between cells (Gladwell and Jefferys, 2001). Variants of gap junctional proteins that respond differently to the same modulators could explain these discrepancies, as could other as yet unidentified sources of electrical coupling, such as pannexin-based junctions.

Therefore, we tested the long-term effects of the AC activator forskolin on electrical synaptic conductance in the TRN. As predicted, forskolin reproduced the effects of DHPG by inducing eLTD (Fig. 4D–F). The coupling strength decreased 4 min after the start of drug application and remained depressed after washout for the duration of the recordings (Fig. 4E, F). Over the entire population of pairs tested with forskolin, electrical coupling strength decreased significantly: $\Delta G_C = -8 \pm 3\%$ ($p = 0.01$, $n = 16$ pairs, two-tailed paired t test; Fig. 4F). Of the 16 cell pairs

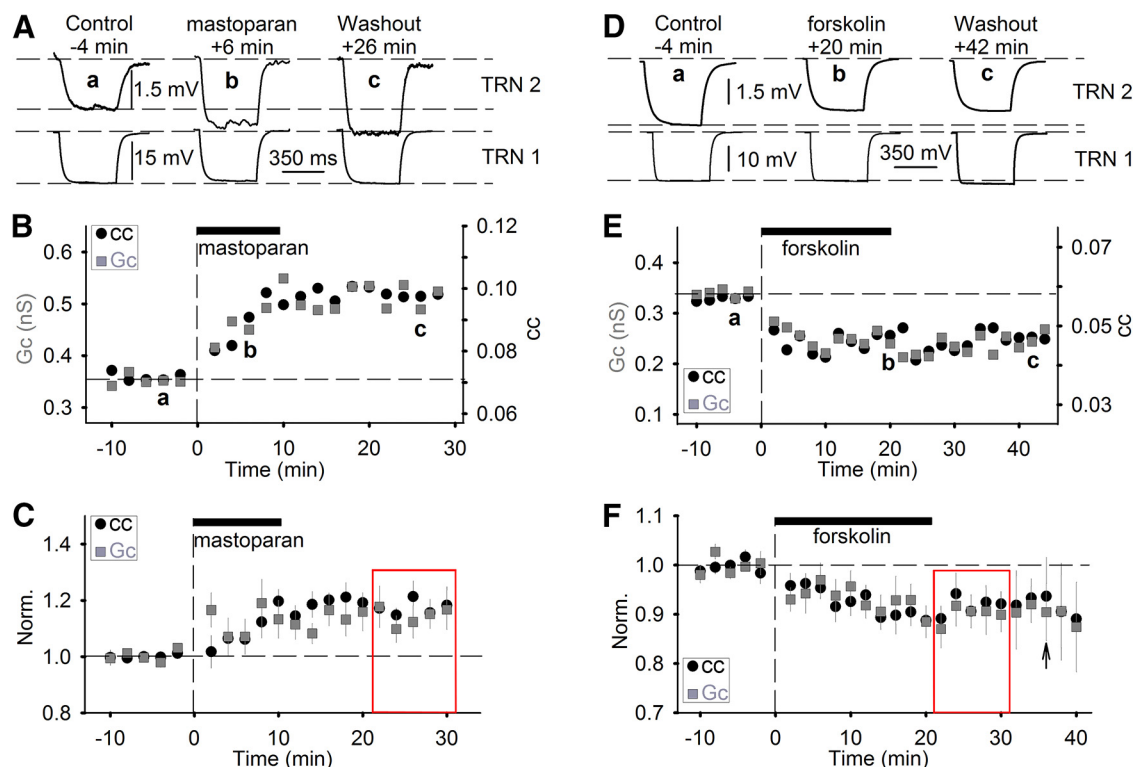


Figure 4. Effects of Gi/o protein activator mastoparan and AC activator forskolin on electrical synaptic coupling strength. **A**, Example single traces of coupled neurons before (a), during (b), and after (c) mastoparan application (2 μ M, 10 min). Stimulation and response parameters as in Figure 2A. **B**, Time course measurements of cc and G_c for the pair of neurons shown in **A** before, during, and after mastoparan application; a–c are the data points corresponding to the traces in **A**. **C**, Normalized population time course of cc and G_c before, during, and after mastoparan application (mean \pm SE; $n = 10$ pairs; cc $p = 0.02$, $G_c p = 0.03$). **D**, Example traces of a single pair of coupled TRN neurons before (a), during (b), and after (c) forskolin application (10 μ M, 20 min). **E**, Time course of cc and G_c for the coupled pair shown in **D**. **F**, Normalized population time course data for cc and G_c before, during, and after forskolin application ($n = 16$ pairs; cc $p = 0.02$, $G_c p = 0.01$). Arrow shows $n = 9$ pairs recorded past 36 min. Red boxes indicate regions of analysis, as in Figures 2 and 3.

tested with forskolin, nine showed significant depression of gap junctional strength. However, it should be noted that forskolin is a cell-permeable compound, which may require additional washout time. In conjunction with our other findings, these results suggest that activation of group I mGluRs can cause the activation of AC intracellularly, and subsequently this activation induces LTD of electrical coupling strength in TRN neurons.

cAMP mediates eLTD

Activation of AC is known to cause an elevation of intracellular cAMP levels. The direct effects of cAMP on electrical coupling strength, however, vary between cell types. Our results show that AC activation induces eLTD in the TRN. Therefore, we reasoned that increasing cAMP directly should also depress electrical coupling strength in the TRN.

To test this hypothesis, we raised cAMP activity by using the cell-permeable cAMP analog 8-bromo-cAMP (8-Br-cAMP). After 8-Br-cAMP application and washout, gap junctional coupling strength rapidly decreased and reached steady-state depression at 20 min after the start of the drug wash (Fig. 5A–C; also see Mitropoulou and Bruzzone, 2003). For all pairs tested with 8-Br-cAMP, electrical coupling strength depressed significantly: $\Delta G_c = -18 \pm 3\%$ ($n = 10$ pairs, $p = 0.0003$; two-tailed paired t test). Together, the above results indicate that activation of the AC–cAMP signaling pathway induces eLTD when triggered by group I mGluRs.

PKA is critical for induction of eLTP

Because the cell-permeable cAMP analog 8-Br-cAMP causes eLTD in TRN, we inferred that an increase in PKA mediates this

effect (Mitropoulou and Bruzzone, 2003; Urschel et al., 2006; Kothmann et al., 2009; Li et al., 2009; Fig. 1D). To verify this relationship, we tested the effect of KT 5720, a potent and selective cell-permeable PKA inhibitor. Application of KT 5720 strongly potentiated the average G_c (Fig. 5D–F; $\Delta G_c = 25 \pm 6\%$, $n = 6$ pairs, $p = 0.02$, two-tailed paired t test), and of the six pairs tested, four showed significant potentiation of gap junctional conductance. It should be noted, however, that since KT 5720 is a cell-permeable compound, it might take extra time for a full washout. But we used a reasonably high flow rate (2 ml/min), so it's likely that these results are indicative of long-term effects.

These results indicate that inhibition of PKA primarily causes eLTP in TRN, which is consistent with results from the activation of group II mGluRs and Gi/o protein. Together, the above results suggest that PKA is a part of the AC–cAMP signaling pathway that regulates long-term modification of electrical synapses in the TRN. Activation or inhibition of any protein in this signaling pathway will induce either potentiation or depression of electrical G_c between TRN neurons. This implies that the state of gap junctional conductance is sensitive to the actual concentration of PKA, since blocking PKA not only prevents eLTD, but also causes eLTP. Thus, activation of group I and group II mGluRs converge on the same signaling cascade (AC–cAMP–PKA) but with opposing results (Fig. 6).

Response heterogeneity

The majority of pairs tested with the agonists and antagonists responded in a consistent fashion, as predicted by the effects of each stage of the signal cascade. However, within each group, we observed a subset of pairs that either showed no significant re-

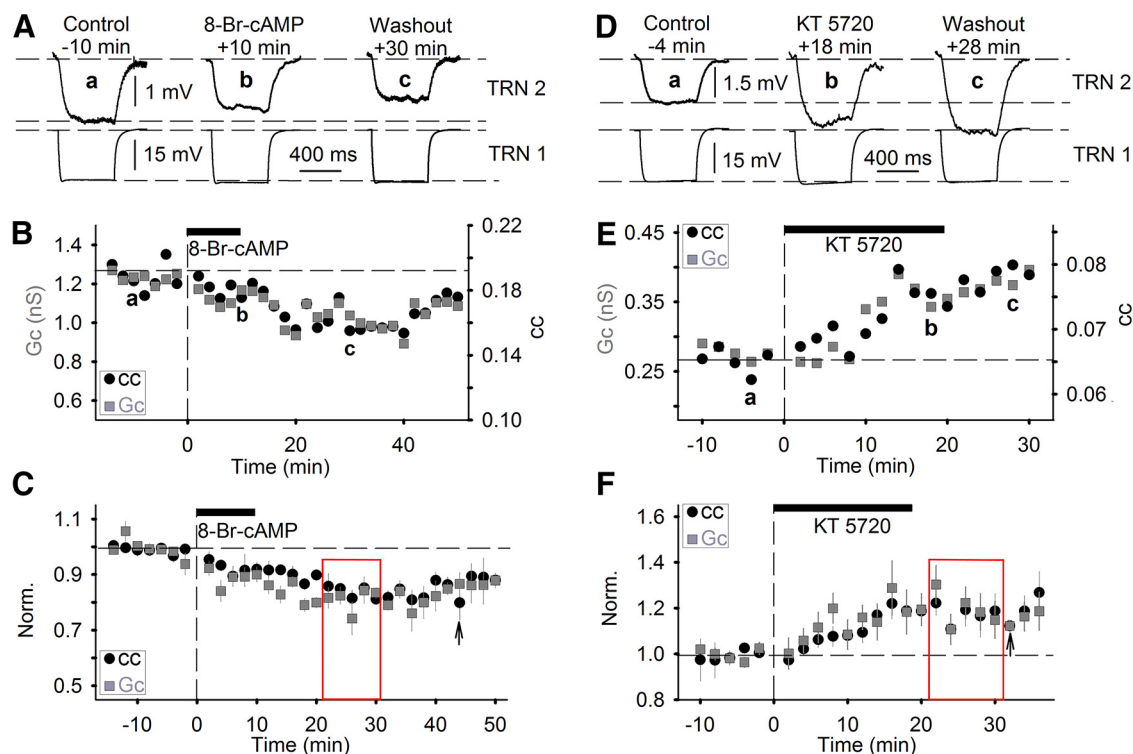


Figure 5. Effects of the cAMP analog 8-Br-cAMP and the PKA inhibitor KT 5720 on electrical synaptic coupling strength. **A**, Single example traces from coupled neurons before (a), during (b), and after (c) 8-Br-cAMP application (2 mM, 10 min); same layout as in Figure 2A. **B**, Time course measurements of cc and G_c for the pair of neurons shown in **A** before, during, and after 8-Br-cAMP application; a–c mark the data time points corresponding to the traces in **A**. **C**, Normalized population time course of cc and G_c before, during, and after 8-Br-cAMP application (mean \pm SE; $n = 10$ pairs; cc $p = 0.0003$, G_c $p = 0.0003$). Arrow indicates $n = 2$ pairs recorded after 44 min. **D**, Single example traces before (a), during (b), and after (c) KT 5720 application (5 μ M, 20 min). Stimulation and response parameters as in Figure 2A. **E**, Time course measurements of cc and G_c for the neuronal pair in **D** (a–c mark the data time points corresponding to the traces in **D**). **F**, Population time course of cc and G_c before, during, and after KT 5720 application (mean \pm SE; $n = 6$ pairs; cc $p = 0.04$, G_c $p = 0.02$).

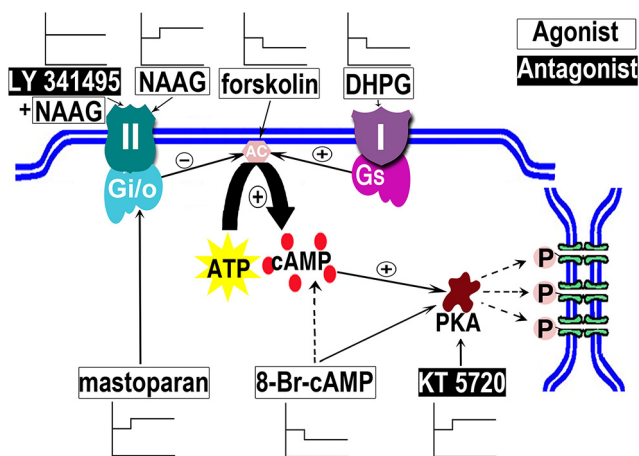


Figure 6. Summary of long-term modification of electrical synaptic coupling strength in TRN via activation of mGluRs and their signaling pathways. Schematic diagram summarizing the findings. Diagram line graphs indicate eLTP, eLTD, or no significant change for the drugs used to test each stage of the signal cascade. Drugs are shown with white backgrounds and black text for agonists and black backgrounds with white text for antagonists for their related receptors or proteins. Membrane-spanning group I mGluRs and group II mGluRs and their associated G-proteins, Gi/o and Gs, are shown as in Figure 1D. Gap junction channels illustrated on the right, in green, in the phosphorylated state (P).

sponse or a response profile opposite to that of the majority of pairs tested (Fig. 7). To determine whether responses were significant for each pair, we used unpaired, one-tailed t tests of the time points 10 min before versus 20–30 min after the start of drug application (see Fig. 2C).

Here we describe the details of the response profiles for each drug tested. Of the 11 pairs tested with the mGluR3 agonist NAAG, only seven (64%) showed significant potentiation (Fig. 7A). G_c increased by $21 \pm 4\%$ for those seven pairs. The remaining four pairs showed no significant response. Of the 11 pairs tested with the group I mGluR agonist DHPG, eight (73%) showed significant depression. For these eight pairs, $\Delta G_c = -32 \pm 4\%$. The remaining three pairs showed no significant responses (Fig. 7B). Eight of 10 (80%) pairs tested with the Gi/o protein activator mastoparan showed significant increases in coupling strength: $\Delta G_c = 25 \pm 6\%$. The remaining two pairs showed no significant change in coupling strength (Fig. 7C).

Of 16 pairs exposed to the AC activator forskolin, nine (56%) pairs showed depression of electrical coupling strength, two pairs showed significant potentiation, and the remaining five pairs exhibited no significant change. For the nine pairs that underwent eLTD in response to forskolin, G_c depressed $19 \pm 3\%$ (Fig. 7D). Four of six pairs (67%) tested with the PKA inhibitor KT 5720 showed potentiated coupling strength ($\Delta G_c = 30 \pm 5\%$), and the remaining two pairs showed no significant changes after drug application (Fig. 7E). Finally, for pairs tested with the cAMP analog 8-Br-cAMP, all 10 pairs underwent significant depression of electrical coupling strength ($\Delta G_c = -18 \pm 3\%$; Fig. 7F). It is unclear whether these variations were due to differences in specificity of the chemicals or due to heterogeneity among neurons within the TRN.

Modification of electrical coupling is inversely related to the baseline coupling strength

To identify what effects contributed to the extent of plasticity between cell pairs, we plotted change in coupling strength after

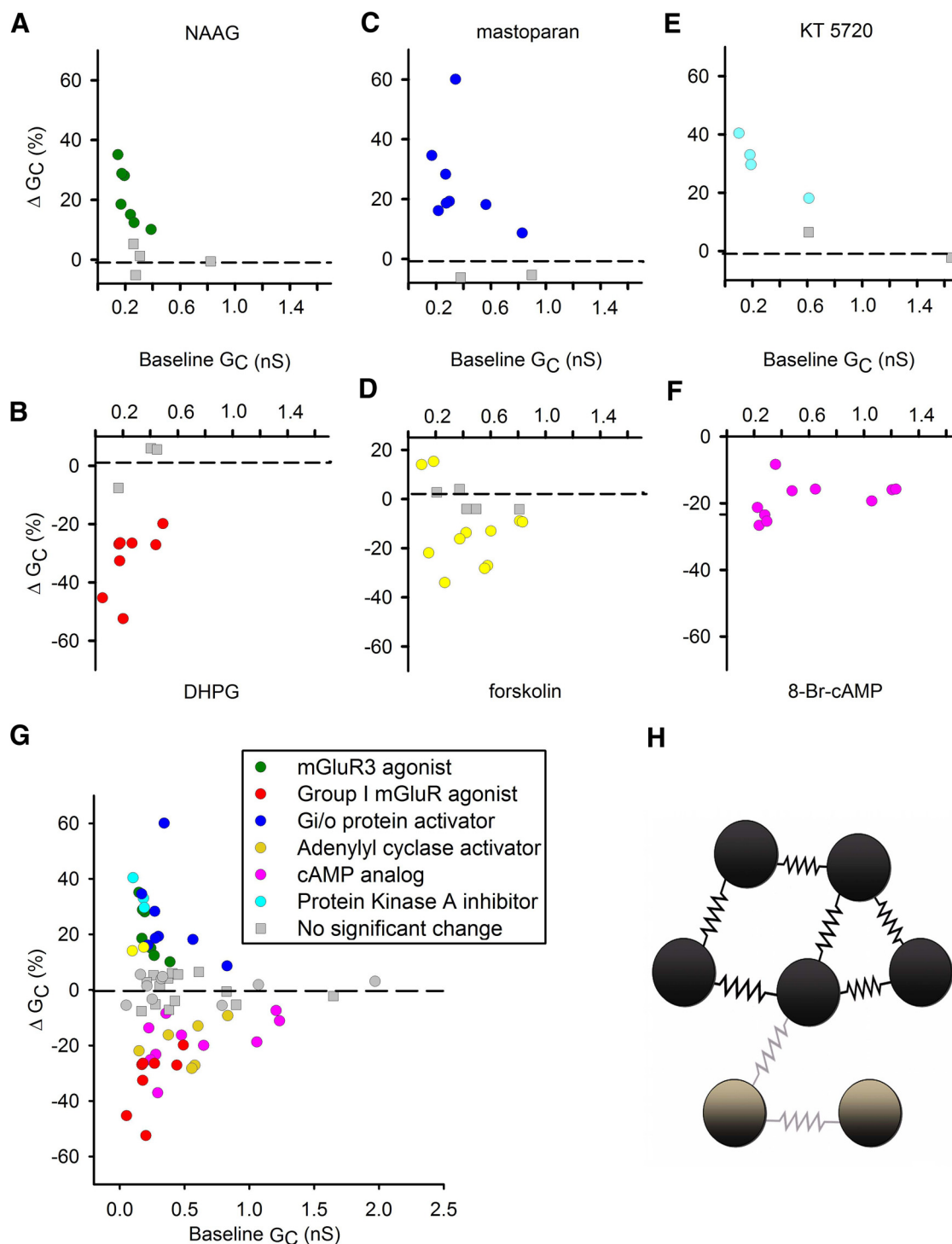


Figure 7. All paired datasets of all pharmacological agents and network schematic. **A–F**, Scatter plots of the percentage change in coupling strength (G_C) for each pair after each drug wash, plotted as a function of baseline coupling strength; pharmacological agents are labeled above and below their respective scatter plots. Gray squares represent pairs with no significant change in coupling strength after drug application. **G**, Combined data from **A–F** for all pharmacological agents. Each dot represents a single recorded pair ($n = 73$ pairs). **H**, Schematic diagram showing an electrically coupled neuronal circuit. Each oval represents a single neuron, and resistor symbols represent electrical synapses. Dark neurons and synapses represent the “scaffolding network,” with strong electrical coupling, which undergo little to no plasticity. The lighter gray neurons and their electrical synapses represent weak to moderate strength synapses that can effectively be added to or subtracted from the gap junctional network via strengthening or weakening of their synapses.

drug application as a function of control baseline coupling strength. For most coupled pairs, baseline G_C varied between 0.15 and 1.2 nS. When the baseline G_C was stronger than 1.2 nS, we never observed significant change after drug application. In fact, the most dramatic changes occurred in the pairs that were most

weakly coupled (Fig. 7G). Thus, the degree of plasticity induced by the various agonists and antagonists is negatively correlated to the baseline coupling strength: the weaker the initial G_C for a pair of electrically coupled neurons, the more likely it is to be significantly modified after drug application.

Discussion

eLTD and eLTP share a common pathway

Long-term modification of synaptic strength by either activity or pharmacological agents has been extensively studied in chemical synapses. In contrast, very few studies have previously shown long-term modification of electrical synapses (eLTP and eLTD) in the mammalian CNS. In the current study, we investigated the underlying mechanisms of eLTD in TRN neurons. We provide the first electrophysiological evidence that electrical synapses in the TRN can also undergo eLTP.

By testing the effects of downstream targets in the AC–cAMP–PKA pathway, we found mechanisms similar to those seen in mGluR-induced long-term modification of chemical synapses (Collingridge et al., 2010; Le Duigou and Kullmann, 2011). Specifically, group I mGluRs induce eLTD, and group II mGluRs induce eLTP. Both mGluR-receptor groups converge on the same intracellular signaling pathway (AC–cAMP–PKA), but have opposing effects on long-term modification of electrical synapses.

eLTD is dominant in TRN, but eLTP can also be expressed

The nonspecific mGluR agonist ACPD induces depolarization of all TRN neurons (Cox and Sherman, 1999; Long et al., 2004; Landisman and Connors, 2005), which is consistent with the effects of group I mGluR agonists alone (Cox and Sherman, 1999) and with the effects of tetanic stimulation of CT feedback fibers (Landisman and Connors, 2005). All three perturbations—ACPD application, group I mGluR agonist application, and stimulation of CT fibers—induce eLTD (Figs. 3, 6; Landisman and Connors, 2005). Thus, despite the high expression profile of mGluR3 (group II) receptors in the TRN (Ohishi et al., 1993; Lourenço Neto et al., 2000; Tamaru et al., 2001), their ability to induce eLTP is greatly overshadowed by the induction of eLTD by group I mGluRs.

There are several possible explanations for these results. First, glutamatergic afferents could activate both groups of receptors, with the final effect depending on the integration of the opposing effects of eLTD and eLTP. This may also explain why some pairs showed no changes after drug application. Second, activation of different mGluRs may require different concentrations of glutamate, different input frequency, or different behavioral states. For instance, group I mGluRs may require a lower level of glutamatergic input than group II mGluRs to induce synaptic modification either in general or in the baseline “state” of the *in vitro* slice. This last hypothesis is supported by the fact that group II mGluRs need higher concentrations of agonists to activate TRN cells recorded in slices (Cox and Sherman, 1999).

G-proteins and the signaling cascades involved in the long-term modification of electrical synapses in the TRN

Both group I and group II mGluRs are capable of influencing the AC–cAMP–PKA signaling pathway. In general, the group II mGluRs couple to Gi/o protein and inhibit cAMP formation (Conn and Pin, 1997; Kim et al., 2008). Specifically, activation of group II mGluRs elevates Gi/o protein activity, which then inhibits the AC–cAMP–PKA signaling cascade, and induces eLTP in TRN neurons. In addition, increasing evidence has shown that group I mGluRs couple to Gs protein to increase AC–cAMP–PKA signal transduction (Bandrowski et al., 2001; Hermans and Challiss, 2001; Lu et al., 2004; Tateyama and Kubo, 2007; Kim et al., 2008). Therefore, it is possible that induction of eLTD in TRN by activation of group I mGluRs results from the Gs–AC–cAMP–

PKA signaling cascade. As a result, the triggering or suppression of AC by activation of group I or group II mGluRs will upregulate or downregulate the activity of the downstream pathway, and consequently induce eLTD or eLTP, respectively (Fig. 6).

Molecular mechanisms involved in the modulation of electrical synapses in the TRN

The Cx36 protein provides most, if not all, of the structural basis for electrical synapses among TRN neurons (Landisman et al., 2002), as well as among other mammalian neurons with a similar biochemical profile (Deans et al., 2001; Galarreta and Hestrin, 2001; Pereda, 2014). However, the mechanism by which PKA affects Cx36 is still not understood. Possible mechanisms include modifying the number of Cx36 channels in the neuronal membrane (Gaietta et al., 2002), regulating channel conductance, and/or changing the probability or duration of the connexin channel open state (McMahon et al., 1989). For most of these mechanisms (except modification of the number of channels), it has been proposed that PKA mediates the direct phosphorylation of Cx36 at its regulatory sites. Kothmann and colleagues (2009) demonstrated that individual gap junctional plaques can have different phosphorylation states, at different regulatory sites, even within a single neuron. The direct phosphorylation of Cx36 has been shown to decrease tracer diffusion in mouse retina (Urschel et al., 2006; Kothmann et al., 2009), as well as decrease current conductance in expressed perch Cx35 hemichannels (the ortholog of rat Cx36; Mitropoulou and Bruzzone, 2003).

The scaffolding network in TRN

GABAergic TRN neurons appear to be electrically coupled locally (<40 μ m) and in relatively small clusters (Long et al., 2004). Calcium imaging reveals that networks of electrically coupled TRN neurons contain ≤ 8 cells (Haas et al., 2011). We found that the modification of electrical coupling is inversely related to baseline coupling strength (Fig. 7G; Szabo et al., 2010). Our hypothesis is that there is a “scaffolding network” of strongly coupled TRN neurons (Fig. 7H). More specifically, even strong depression of a strongly coupled pair will not eliminate the synchrony of these neurons within their electrically coupled network. This would explain why strongly coupled pairs underwent little to no observable modulation (Fig. 7). Thus, the scaffolding of a coupled network is composed of these strongly coupled neurons that provide a local anchor for more weakly coupled neurons. When the electrical synapses of these weakly coupled cells are positively modulated/potentiated, these cells can synchronize their activity with the activity of the scaffolding network. Conversely, when these weaker synapses are negatively modulated/depressed, their affiliated neurons functionally leave the synchronized network because their synapses are no longer strong enough to correlate their activity to the scaffolding cells. Thus, the weaker players can actually leave or join the network based on their plastic responses, eLTD or eLTP, respectively. Because one TRN neuron alone can inhibit ≥ 100 relay cells (McCormick and Contreras, 2001), whether or not these coupled pairs are part of a synchronized network can influence the activity of thousands of relay cells within the TC system.

The potential function of modulation of electrical synapses in TRN

If the thalamus is considered the gateway to the cerebral cortex, then the TRN is the guardian of that gateway, due to its central role in regulating TC interactions (Crick, 1984). The TRN is known to participate in TC oscillations during many conditions,

including sleep (sleep spindle rhythms), vigilance, and attention (Llinás and Jahnsen, 1982; Deschênes et al., 1984; Jahnsen and Llinás, 1984; Steriade et al., 1987). In the TRN, electrical synapses are common among compact clusters of neurons, and they synchronize the activity among these coupled neurons (Landisman et al., 2002; Long et al., 2004; for review, see Bennett and Zukin, 2004; Connors and Long, 2004; Cruikshank et al., 2005). The low-pass filter characteristics associated with electrical synapses (Landisman et al., 2002; Long et al., 2004; Gibson et al., 2005; for explanation see Söhl et al., 2005) regulate the transduction of subthreshold rhythmic oscillations. We have demonstrated previously that low-frequency, subthreshold oscillations can be induced by nonspecific activation of mGluRs (Long et al., 2004).

Therefore, modification of electrical coupling in the TRN potentially plays an important role in state-dependent modification of the temporal and spatial transmission of information within the TC system. In states of low sensory input, such as during sleep, activation of group I mGluRs could induce eLTD. This would then allow the feed-forward and feedback chemical synaptic drive to control synchrony in the thalamocortical system. In contrast, eLTP would presumably be induced by relatively higher frequency patterns of inputs occurring during periods of selective attention. Thus, the functions of inhibition generated in the TRN almost certainly undergo dynamic changes as a result of the dynamic plasticity of their gap junctional synapses.

References

- Agmon A, Connors BW (1991) Thalamocortical responses of mouse somatosensory (barrel) cortex in vitro. *Neuroscience* 41:365–379. [CrossRef Medline](#)
- Alexander GM, Godwin DW (2005) Presynaptic inhibition of corticothalamic feedback by metabotropic glutamate receptors. *J Neurophysiol* 94:163–175. [CrossRef Medline](#)
- Alexander GM, Godwin DW (2006) Unique presynaptic and postsynaptic roles of group II metabotropic glutamate receptors in the modulation of thalamic network activity. *Neuroscience* 141:501–513. [CrossRef Medline](#)
- Bandrowski AE, Ashe JH, Crawford CA (2001) Tetanic stimulation and metabotropic glutamate receptor agonists modify synaptic responses and protein kinase activity in rat auditory cortex. *Brain Res* 894:218–232. [CrossRef Medline](#)
- Bennett MV (1966) Physiology of electrotonic junctions. *Ann N Y Acad Sci* 137:509–539. [CrossRef Medline](#)
- Bennett MV, Zukin RS (2004) Electrical coupling and neuronal synchronization in the mammalian brain. *Neuron* 41:495–511. [CrossRef Medline](#)
- Collingridge GL, Peineau S, Howland JG, Wang YT (2010) Long-term depression in the CNS. *Nat Rev Neurosci* 11:459–473. [CrossRef Medline](#)
- Conn PJ, Pin JP (1997) Pharmacology and functions of metabotropic glutamate receptors. *Annu Rev Pharmacol Toxicol* 37:205–237. [CrossRef Medline](#)
- Connors BW, Long MA (2004) Electrical synapses in the mammalian brain. *Annu Rev Neurosci* 27:393–418. [CrossRef Medline](#)
- Coutinho V, Knöpfel T (2002) Metabotropic glutamate receptors: electrical and chemical signaling properties. *Neuroscientist* 8:551–561. [CrossRef Medline](#)
- Cox CL, Sherman SM (1999) Glutamate inhibits thalamic reticular neurons. *J Neurosci* 19:6694–6699. [Medline](#)
- Crabtree JW (1999) Intrathalamic sensory connections mediated by the thalamic reticular nucleus. *Cell Mol Life Sci* 56:683–700. [CrossRef Medline](#)
- Crick F (1984) Function of the thalamic reticular complex: the searchlight hypothesis. *Proc Natl Acad Sci U S A* 81:4586–4590. [CrossRef Medline](#)
- Cruikshank SJ, Landisman CE, Mancilla JG, Connors BW (2005) Connexon connexions in the thalamocortical system. *Prog Brain Res* 149:41–57. [CrossRef Medline](#)
- Deans MR, Gibson JR, Sellitto C, Connors BW, Paul DL (2001) Synchronous activity of inhibitory networks in neocortex requires electrical synapses containing connexin36. *Neuron* 31:477–485. [CrossRef Medline](#)
- Deleuze C, Huguenard JR (2006) Distinct electrical and chemical connectivity maps in the thalamic reticular nucleus: potential roles in synchronization and sensation. *J Neurosci* 26:8633–8645. [CrossRef Medline](#)
- Deschênes M, Paradis M, Roy JP, Steiade M (1984) Electrophysiology of neurons of lateral thalamic nuclei in cat: resting properties and burst discharges. *J Neurophysiol* 51:1196–1219. [Medline](#)
- Fuhrman S, Palkovits M, Cassidy M, Neale JH (1994) The regional distribution of N-acetylaspartylglutamate (NAAG) and peptidase activity against NAAG in the rat nervous system. *J Neurochem* 62:275–281. [Medline](#)
- Gaietta G, Deerinck TJ, Adams SR, Bouwer J, Tour O, Laird DW, Sosinsky GE, Tsien RY, Ellisman MH (2002) Multicolor and electron microscopic imaging of connexin trafficking. *Science* 296:503–507. [CrossRef Medline](#)
- Galarreta M, Hestrin S (2001) Electrical synapses between GABA-releasing interneurons. *Nat Rev Neurosci* 2:425–433. [CrossRef Medline](#)
- Gibson JR, Beierlein M, Connors BW (2005) Functional properties of electrical synapses between inhibitory interneurons of neocortical layer 4. *J Neurophysiol* 93:467–480. [Medline](#)
- Gladwell SJ, Jefferys JG (2001) Second messenger modulation of electrotonic coupling between region CA3 pyramidal cell axons in the rat hippocampus. *Neurosci Lett* 300:1–4. [CrossRef Medline](#)
- Golshani P, Warren RA, Jones EG (1998) Progression of change in NMDA, non-NMDA, and metabotropic glutamate receptor function at the developing corticothalamic synapse. *J Neurophysiol* 80:143–154. [Medline](#)
- Haas JS, Zavala B, Landisman CE (2011) Activity-dependent long-term depression of electrical synapses. *Science* 334:389–393. [CrossRef Medline](#)
- Hampson EC, Vaney DI, Weiler R (1992) Dopaminergic modulation of gap junction permeability between amacrine cells in mammalian retina. *J Neurosci* 12:4911–4922. [Medline](#)
- Henderson Z, Salt TE (1988) The effects of N-acetylaspartylglutamate and distribution of N-acetylaspartylglutamate-like immunoreactivity in the rat somatosensory thalamus. *Neuroscience* 25:899–906. [CrossRef Medline](#)
- Hermans E, Challiss RA (2001) Structural, signaling and regulatory properties of the group I metabotropic glutamate receptors: prototypic family C G-protein coupled receptors. *Biochem J* 359:465–484. [Medline](#)
- Hughes SW, Crunelli V (2006) Hardwiring goes soft: long-term modulation of electrical synapses in the mammalian brain. *Cellscience* 2:1–9. [Medline](#)
- Jahnsen H, Llinás R (1984) Voltage-dependent burst-to-tonic switching of thalamic cell activity: an in vitro study. *Arch Ital Biol* 122:73–82. [Medline](#)
- Kim CH, Lee J, Lee JY, Roche KW (2008) Metabotropic glutamate receptors: phosphorylation and receptor signaling. *J Neurosci Res* 86:1–10. [Medline](#)
- Kolodziejczyk K, Hamilton NB, Wade A, Kárádóttir R, Attwell D (2009) The effect of N-acetyl-aspartyl-glutamate and N-acetyl-aspartate on white matter oligodendrocytes. *Brain* 132:1496–1508. [CrossRef Medline](#)
- Kothmann WW, Massey SC, O'Brien J (2009) Dopamine-stimulated dephosphorylation of connexin 36 mediates AII amacrine cell uncoupling. *J Neurosci* 29:14903–14911. [CrossRef Medline](#)
- Landisman CE, Connors BW (2005) Long-term modulation of electrical synapses in the mammalian thalamus. *Science* 310:1809–1813. [CrossRef Medline](#)
- Landisman CE, Long MA, Beierlein M, Deans MR, Paul DL, Connors BW (2002) Electrical synapses in the thalamic reticular nucleus. *J Neurosci* 22:1002–1009. [Medline](#)
- Le Duigou C, Kullmann DM (2011) Group I mGluR agonist-evoked long-term potentiation in hippocampal oriens interneurons. *J Neurosci* 31:5777–5781. [CrossRef Medline](#)
- Li H, Chuang AZ, O'Brien J (2009) Photoreceptor coupling is controlled by connexin 35 phosphorylation in zebrafish retina. *J Neurosci* 29:15178–15186. [CrossRef Medline](#)
- Llinás R, Jahnsen H (1982) Electrophysiology of mammalian thalamic neurons in vitro. *Nature* 297:406–408. [CrossRef Medline](#)
- Long MA, Landisman CE, Connors BW (2004) Small clusters of electrically coupled neurons generate synchronous rhythms in the thalamic reticular nucleus. *J Neurosci* 24:341–349. [CrossRef Medline](#)
- Lourenço Neto F, Schadrack J, Berthele A, Zieglgänsberger W, Tölle TR, Castro-Lopes JM (2000) Differential distribution of metabotropic glutamate receptor subtype mRNAs in the thalamus of the rat. *Brain Res* 854:93–105. [Medline](#)
- Lu D, Yan H, Othman T, Rivkees SA (2004) Cytoskeletal protein 4.1G is a binding partner of the metabotropic glutamate receptor subtype 1 alpha. *J Neurosci Res* 78:49–55. [Medline](#)

- McCormick DA, Contreras D (2001) On the cellular and network bases of epileptic seizures. *Annu Rev Physiol* 63:815–846. [CrossRef Medline](#)
- McLean HA, Caillard O, Khazipov R, Ben-Ari Y, Gaiarsa JL (1996) Spontaneous release of GABA activates GABA_B receptors and controls network activity in the neonatal rat hippocampus. *J Neurophysiol* 76:1036–1046. [Medline](#)
- McMahon DG, Knapp AG, Dowling JE (1989) Horizontal cell gap junctions: single-channel conductance and modulation by dopamine. *Proc Natl Acad Sci U S A* 86:7639–7643. [CrossRef Medline](#)
- Mitropoulou G, Bruzzone R (2003) Modulation of perox connexin35 hemichannels by cyclic AMP requires a protein kinase A phosphorylation site. *J Neurosci* 23:147–157. [Medline](#)
- Moffett JR, Namboodiri AM (2006) Expression of N-acetylaspartate and N-acetylaspartylglutamate in the nervous system. *Adv Exp Med Biol* 576:7–26; discussion 361–363. [Medline](#)
- Ohishi H, Shigemoto R, Nakanishi S, Mizuno N (1993) Distribution of the mRNA for a metabotropic glutamate receptor (mGluR3) in the rat brain: an in situ hybridization study. *J Comp Neurol* 335:252–266. [Medline](#)
- Pereda AE (2014) Electrical synapses and their functional interactions with chemical synapses. *Nat Rev Neurosci* 15:250–263. [CrossRef Medline](#)
- Pin JP, Acher F (2002) The metabotropic glutamate receptors: structure, activation mechanism and pharmacology. *Curr Drug Targets CNS Neurol Disord* 1:297–317. [Medline](#)
- Rörig B, Klaus G, Sutor B (1995) Dye coupling between pyramidal neurons in developing rat prefrontal and frontal cortex is reduced by protein kinase A activation and dopamine. *J Neurosci* 15:7386–7400. [Medline](#)
- Scheibel ME, Scheibel AB (1966) Terminal axonal patterns in cat spinal cord. I. The lateral corticospinal tract. *Brain Res* 2:333–350. [Medline](#)
- Shpakov AO, Pertseva MN (2006) Molecular mechanisms for the effect of mastoparan on G proteins in tissues of vertebrates and invertebrates. *Bull Exp Biol Med* 141:302–306. [Medline](#)
- Söhl G, Maxeiner S, Willecke K (2005) Expression and functions of neuronal gap junctions. *Nat Rev Neurosci* 6:191–200. [Medline](#)
- Steriade M, Domich L, Oakson G, Deschênes M (1987) The deafferented reticular thalamic nucleus generates spindle rhythmicity. *J Neurophysiol* 57:260–273. [Medline](#)
- Steriade M, Jones EG, McCormick DA (1997) *Thalamus. Organization and function*. Amsterdam: Elsevier.
- Szabo TM, Caplan JS, Zoran MJ (2010) Serotonin regulates electrical coupling via modulation of extrajunctional conductance: H-current. *Brain Res* 1349:21–31. [CrossRef Medline](#)
- Tamaru Y, Nomura S, Mizuno N, Shigemoto R (2001) Distribution of metabotropic glutamate receptor mGluR3 in the mouse CNS: differential location relative to pre- and postsynaptic sites. *Neuroscience* 106:481–503. [CrossRef Medline](#)
- Tateyama M, Kubo Y (2007) Coupling profile of the metabotropic glutamate receptor 1alpha is regulated by the C-terminal domain. *Mol Cell Neurosci* 34:445–452. [Medline](#)
- Urschel S, Höher T, Schubert T, Alev C, Söhl G, Wörsdorfer P, Asahara T, Dermietzel R, Weiler R, Willecke K (2006) Protein kinase A-mediated phosphorylation of connexin 36 in mouse retina results in decreased gap junctional communication between AII amacrine cells. *J Biol Chem* 281:33163–33171. [Medline](#)
- Westbrook GL, Mayer ML, Namboodiri MA, Neale JH (1986) High concentrations of N-Acetylaspartylglutamate (NAAG) selectively activate NMDA receptors on mouse spinal cord neurons in cell culture. *J Neurosci* 6:3385–3392. [Medline](#)
- Zsiros V, Maccaferri G (2008) Noradrenergic modulation of electrical coupling in GABAergic networks of the hippocampus. *J Neurosci* 28:1804–1815. [CrossRef Medline](#)